Analysis of Kinetics and Efficacy of Anti-Cancer via Oxygen-Enhanced Photodynamic Therapy

Jui-Teng Lin[1,*], Kuo-Ti Chen[2] and Hsia-Wei Liu[2,3]

[1]*New Vision Inc. Taipei, Taiwan*

[2]*Graduate Institute of Applied Science and Engineering, Fu Jen Catholic University, New Taipei City, Taiwan*

[3]*Department of Life Science, Fu Jen Catholic University, New Taipei City, Taiwan*

Abstract: Photodynamic therapy (PDT has been widely used in many medical applications. PDT for anti-cancer is one of the clinically important subjects. This study will analyze the photochemical kinetics and the efficacy of anti-cancer via the critical factors including: the concentrations of photosensitizers and oxygen in the treated target, the exposure time, intensity and does (energy) of the light applied to the target. To achieve high efficacy, one requires the oxygen source term to re-supply the depletion of oxygen and photosensitizers. Higher light intensity has faster rising curve of the efficacy, but it reaches the same steady-state value as that of low intensity. The efficacy follows the Bunsen-Roscoe law (BRL) of reciprocity only when there is no oxygen source term. Higher initial concentration of oxygen and photosensitizers, C_0, always provide higher efficacy. To achieve the same efficacy, minimum dose and/or less exposure time for accelerated procedure may be achieved by using a higher intensity (but same dose) for the case of P=0. However, with P>0, higher intensity requires a higher fluence to achieve the same efficacy and it does not follow the BRL reciprocity law.

Keywords: Photodynamic therapy, Cancer therapy, Photosensitizers, Reactive oxygen species, Cell viability, Threshold dose, Modeling.

INTRODUCTION

Photo-biological processes (PBP) can be performed by various lasers ranging from ultraviolet to near-infrared [1]. PBP can be either thermal (heating) or non-thermal (chemical) and its efficacy depends on the optical properties of the targeted tissues and photosensitizers, and the light parameters such as its wavelength, energy, intensity, pulse-width, repetition rate and the operation modes. To improve the PBP efficacy nanoparticles (NPs) have been used to cause tumor cell death by photothermal ablation, photodynamic toxicity, mechanical damage, or increase in the localized drug concentration [1]. Moreover, using surface plasmon resonance (SPR) in various shapes of gold nanoparticles (GNP), such as spheres, rods, boxes, cages and shells have been developed, and changing the shape of GNP from spheres to nanorods, the absorption and scattering peaks change from visible to the near-infrared (NIR) regime [1,2].

Comparing to the visible light, light in the NIR regime offers the advantages of larger absorption and scattering cross sections and much deeper penetration depth in tissues. Lin *et al*. [2] proposed the use of a near IR diode laser system having multiple wavelengths for more efficient treatment of cancer tumor. To overcome the penetration issue, Lin *et al*. [2] also proposed the use of a train-pulse to increase the volume temperature increase which is particularly useful to larger volume tumors, unless an inserting fiber is used to deliver the laser energy.

NPs for dual-modality of fluorescence and magnetic resonance imaging-guided, and dual-therapy using photothermal therapy (PTT) and photodynamic therapy (PDT) have been developed recently [3-6]. Dual-modality provides a powerful tool for combining diagnosis and therapy in one system, whereas combined PTT/PDT provides synergic treatment modalities to overcome current limitations of PDT, thus achieving enhanced anticancer efficacy.

As shown in Figure **1**, factors influencing the efficacy of PDT include: selectivity, penetration and optimization, where maximum light penetration depth and efficacy, minimum dose (or treatment time), and high selectivity are desired. However, minimum treatment time and maximum therapy efficacy are two competing factors and can not be easily overcome. Optimal combination of light energy (dose), intensity and irradiation time may be achieved via Lin-scaling laws, Arndt-Schulz-Law (for therapeutic window) and Bunsen-Roscoe law (for reciprocity rule) [7]. Bunsen-Roscoe law (BRL) of reciprocity stating that the effect of a photo-biological reaction is proportional only to the total irradiation fluence (or light dose) (E=It), or the product of intensity (I) and exposure time (t). To achieve the same efficacy, the required exposure time

*Address correspondence to this author at the New Vision Inc. Taipei, Taiwan; E-mail: jtlin55@gmail.com

ISSN: 1929-2260 / E-ISSN: 1929-2279/18

based on BRL is given by t=E/I. Based on BRL, treatment time may be shortened by using a higher intensity while maintaining the similar efficacy. However, BRL is still controversial and has limited validation, as reported by Lin [7].

Oxygen plays a critical role in the efficacy of Type-II PDT [8-13], where oxygen consumption and diffusion effects in PDT was first reported by Foster *et al.* [9] in 1991 and was updated and reviewed recently by Zhu at al [13] in 2017. The kinetics of both oxygen-mediated (type-II) and non-oxygen-mediated (type-I) was reported by Lin recently [8]. For ophthalmic applications, the reciprocity law was reported for the role of drug-light dose on the PDT efficacy [14-17]. PDT for was theoretically studied for cancer therapy [9-13], and more recently by Lin [8] for corneal deceases which will be revised for cancer therapy in this study.

In this study, we will analyze the efficacy of anti-cancer via oxygen-enhanced type-II photodynamic therapy. Generation of reactive oxygen species (ROS), the depletion times and resupply of photosensitizer and/or oxygen will be analyzed. Minimum light dose and/or less exposure time for accelerated procedure by using a higher intensity (but same dose, E_0) are desired. We will show that a threshold product of $[C_0E_0]^*$ and larger C_0 has a lower threshold energy E_0^*. We will demonstrate that, without the oxygen resupply term, the PDT efficacy follows the Bunsen-Roscoe law (BRL) of reciprocity. However, non-BRL is found when there is oxygen resupply term. This new finding in this study and will provide useful clinical guidance for fast and effective anti-cancer PDT.

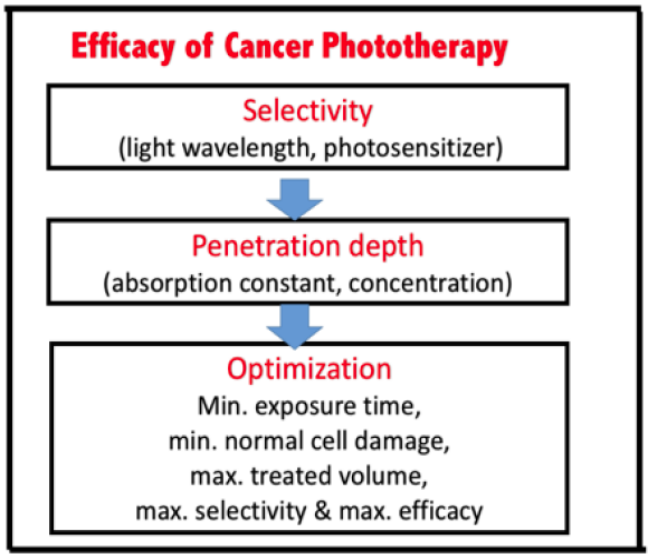

Figure 1: Summary of factors influencing the efficacy of PDT for anti-cancer.

KINETICS OF PHOTODYNAMIC THERAPY

PDT makes use of photosensitizers (PS) to generate reactive reactive species upon the absorption of specific wavelengths of light, where the selectivity is given by: (i) PSs are preferentially taken up by tumour tissues, and (ii) the molecules generate cytotoxic radical species only at the site where light is administered. There are two cytotoxic photochemical mechanisms in PDT (as shown by Figure **2**): (i) Type-I mechanism where the molecule directly reacts through its triplet excited state to generate reactive radicals species; and (ii) Type –II mechanism where PSs convert molecular oxygen into highly reactive singlet oxygen. Most PSs currently used in the clinic are predominantly oxygen-mediated Type –II molecules. It is also possible that both Type-I and –II coexist.

Depending on the target site, PDT effects include destruction of blood vessels, killing of tumour tissue and cells, and induction of immune response. If the PS is also mainly retained in the blood vessels, the type-II process produced singlet oxygen (SO) can damage the blood vessels, causing insufficient blood supply to the lesion, indirectly cause cell death. When the PS reaches the cell, SO may lead to cell apoptosis, necrosis and autophagy. The path of death depends on the concentration and distribution of SO in the course of treatment. In addition, many studies have shown that PDT for tumor cells itself has a strong immunogenicity and can stimulate the specific immune response, where the patient's active immune response to the tumor and can be automatically removed without irradiation.

Most PS available for PDT utilizes Type II photodynamic processes, i.e., the photodynamic effect is achieved through the production of singlet oxygen [8,13]. As shown in Figure **2**, the process begins with the absorption of a photon by PS in its ground state, promoting it to an excited state. The PS molecule can return to its ground state by emission of a fluorescence photon, or convert to a triplet state which may undergo a collisional energy transfer with ground state molecular oxygen (type II process), or with the substrate/target (type I process). In type II interaction, the PS returns to its ground state, and oxygen is promoted from its ground state (a triplet state) to its excited (singlet) state. In type-II process, the PS is almost not consumed (due to the slow singlet oxygen quenching rate), whereas in type-I process the PS is largely depleted specially for high intensity [8].

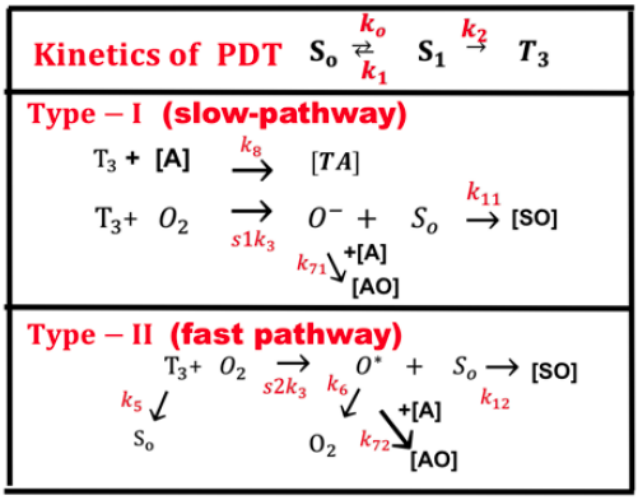

Figure 2: The kinetics of PDT showing both type-I and type-II pathways [8].

The life time of the singlet and triplet states of photosensitizer and the singlet oxygen are very short (ns to μs time scale) since they either decay or react with cellular targets immediately after they are created, therefore, a set of quasi-steady state macroscopic kinetic equation for the concentration of the ground state PS, C (z, t), the ground state oxygen, $[O_2]$, the target substrate, [A], and the light intensity, I (z, t), are given by [8,13]

$$\frac{\partial C(z,t)}{\partial t} = -b(g[A] + g')C \tag{1.a}$$

$$\frac{\partial [O_2]}{\partial t} = -b[s_1 + s_2 K]G + P \tag{1.b}$$

$$\frac{\partial [A]}{\partial t} = -b[gC + K'G][A] \tag{1.c}$$

$$\frac{\partial I(z,t)}{\partial z} = -A'(z,t)I(z,t) \tag{1.d}$$

where b=aqI (z, t); g=(k_8/k_3) G_0; g'=K_{12}(C+d') $[O_2]$ G_0, G=C$[O_2]$ G_0; G_0=/($[O_2]$ +k+L), k=k_5/k_3; L=(k_8/k_3) [A]; K= k_{72}[A]/K_2; K'=(s_1+s_2) k_{72}/K_2; K_{12}= $(s_1k_{11}/K_1 + s_2k_{12}/K_2)$; K_1= k_{11}(C+d') +k_{71}[A]; K_2= k_6 +k_{12}(C+d') +k_{72}[A]; a is a coupling constant; q is the triplet state [T] quantum yield given by q=$k_2/(k_1+k_2)$; s_2 and s_1 are the fraction of $[O_2]$ converted to the singlet oxygen and other ROS, respectively, in type-II and type-I;

d' is a low concentration correction to count for the limited diffusion distance of the reactive species [13], it can be treated as the C-independent quenching rate of ROS. We have also included in Eq. (1.b) the oxygen source term P (z, t) =p(1-$[O_2]$/ $[O_2]_0$), with a rate constant p to count for the situation when there is an external continuing supply, or nature replenishment (at a rate of p), besides the initial oxygen in the stroma. Eg. (1.d) defines the dynamic light intensity including the effect due to depletion of C (z, t) due to light intensity, with an effective absorption coefficient given by A' (z, t) =a'C (z, t), which in general is time and z-dependent [8], but can be approximated by it time-averaged mean value of A'(z)=0.3C_0(1-0.25z/D), (1/uM/cm), such that the light intensity is reduced to about 1/e=0.36, at z=0.5cm and for C_0=8.5 uM; where D is the diffusion depths of photosensitizer.

The above coupled equations will be solved under initial conditions having initial profiles defined by their diffusion depths, D (for photosensitizer), D' (for oxygen), and 2D (for light intensity, given by C_0(z)=1-0.5z/D, $[O_0]$ (z)=1-0.5z/D, and I_0(z)=1-0.5z/ (2D), respectively. For uniform case, D>>1 and D'>>1 cm, and we will consider D and D' in the range of 0,3 to 0.5 cm to count for the non-uniform profiles of the photosensitizer and oxygen.

In the above quasi-steady state, the singlet oxygen concentration of the reactive oxygen species (ROS) are given by: [O'] =bs_1K_1G, for the superoxide anion; and [$^1O_2$] =bs_2K_2G, for the singlet oxygen. [O'] and [$^1O_2$] represent, respectively, the amounts of reactive oxygen species (ROS) in type-I and type-II mechanism.

We note that Eq. (1) reduces to that of Zhu *et al.* [13] for the following simplified situations: k_{72}/K_2 is approximated by 1 with no [A] dependence in K' and K_{12}, such that there is no need to solve for Eq. (1.c); constant diffusion profile of C (z, t), with D>>1; and type-I term (g) is ignored. Therefore, our Eq. (1) is much more accurate than Zhu *et al*. Moreover, all previous modeling [9-13] only solve for numerical results which lost most of the available analysis for physical and chemical processes in this study. Moreover, the anti-cancer efficacy (in this study) is given by Eff=1-exp(-S1+S2), with S1 and S2 are the S-function (for type-I and type-II) given by the time-integral of bgC and bK'G, respectively, for type-I an d-II, based on Eq. (1.c); whereas, Eff=S2, under the assumption of Zhu *et al.* [13], which assumed K'G[A]=G, independent to [A].

$$S1 = \int_0^t bgC(z,t)\,dt \tag{2.a}$$

$$S2 = f\int_0^t bK'G\,dt \tag{2.b}$$

Where f is the fraction of ROS interacting with [A]. Here, S2 relates to the fraction of acceptors that reacted due to (ROS)-mediated reactions, and S1 relates to the fraction that reacts under hypoxic conditions or any other non-oxygen-mediated reactions, such as triplet interactions.

Given the efficacy, Eff = 1 – exp[-(S1+S2)], one may obtain the cancer cells viability (%) defined by CV=1-Eff=exp[-(S1+S2)], which can be compared to measured data. One may also calculate the threshold of cumulated singlet oxygen concentration, defined by when CV< 0.36, or (S1+S2)>1.0.

A complete numerical simulation will be shown elsewhere and we will focus on the roles of each of the key parameters in both type-I and type-II PDT. Typical values of the parameters to be used in our calculations are (referred to Zhu *et al.* [13]: Initial values: C_0=8.5 uM, $[^3O_2]_0$=83 uM, k=k_5/k_3=11.9; $k_{11}=k_{12}$; k_6/k_{12}=1,000. Other parameters d', $k_{83}=(k_8/k_3)$, $[A]_0$, b=aqI_0, will have ranges such that type-I and type-II contributions are different.

RESULTS AND DISCUSSIONS

For type-II dominant case, with g<<g', the first-order solution of Eq. (1.a) gives C (z, t) =C_0exp(-b't), with b'=bKd', which is used to solve for Eq. (1.b), the oxygen concentration $[O_2]$ =X (z, t) is given by the following nonlinear equation (for P=0): X+klnX=X_0+klinX_0 – bC_0[1-exp(-b't)]/b', which maybe sued to fid the second order solution of C (z, t) =C_0exp(-Bt), with B=b'+(k/X_{00}) (1+0.5b't), X_{00}= X_0+klinX_0. The type-II S-function, S2, is given by the time integral of the singlet oxygen, or the integral of, eq. (2.b), bK'G=bK'(C+d') X/(X+11.9+0.65[A]), which is proportional to the product of $C_0X_0E_0$ with E_0=tI_0 being the light fluence (dose).

The approximated analytic formula for S2 is given by: S2=(fbK'C_0/b') [1-exp(-b't)] [1-k/X_{00}]. This formula provides us the following important features: (a) for transient state, with b't<<1, [1-exp(-b't)]/b' = t (1-0.5b't +.), and S2 (at z=0) =aqfK'C_0E_0(1-0.5aqE_0), so that S2 proportional to the product of C_0E_0, and follows the Bunsen-Roscoe law (BRL) of reciprocity; (b) for steady-state, 1-exp(-b't) =1, S (at z=0) = C_0K'/K, which is independent to light intensity and proportional to the initial photosensitizer concentration, C_0. The transient S also defines the threshold of cumulated singlet oxygen concentration, defined by when CV< 0.36, or S2>S2*=1.0, which defines the threshold product of aqfK'C_0E_0(1-0.5aqE_0) =1.0, or $[C_0E_0]$*>1/[aqfK']. Therefore, larger C_0 has a lower E_0* and vice versa.

Depletion Time

As shown by Eq. (2.b), the type-II S-function, S2, is proportional to the time integral over C$[O_2]G_0$, which is proportional to the time profile of the oxygen $[O_2]$ and the photosensitizer concentration, C(z,t). Therefore, it is also governed by their depletion time (T1 and T2), defined by when they reduced to $1/e^2$ = 0.133 of the initial value. By the approximated C(z,t)=C_0exp(-Bt), we obtain, for photosensitizer, T1=2/B=2/(g[A]+g'). Similarly, for oxygen, T2=0.87X_{00}/(bC_0). S2 and type-II efficacy (Eff) reach their steady-state when either $[O_2]$ or C(z,t) is 100% depleted, or 87% depleted at the depletion time (T1 or T2, whatever is smaller). The depletion times are governed by the parameters of aqI, g[A] and g', which in turn are governed by I_0, $[A]_0$ and the rate constants $k_{83}=k_8/k_3$. both T1 and T2 are decreasing function of the light intensity, that is higher intensity has smaller T1 and T2, whereas it has faster rising profile of the S-functions.

Figures **3**, **4**, **5** and **6** show the time profiles of oxygen, $[O_2]$, and photosensitizer concentration, C(z,t), and S2, for various light intensity of I_0= (50,100, 200) mW/cm^2, where we have used parameters of initial values: C_0=8.5 uM, $[^3O_2]_0$=83 uM, d'=33 uM; k=k_5/k_3=11.9. Other parameters; k_6/k_{12}=1,000, $k_{83}=(k_8/k_3)$=0.0001, b'=aq=0.03, $[A]_0$=50 uM, for the case of P=0 (no oxygen supply).

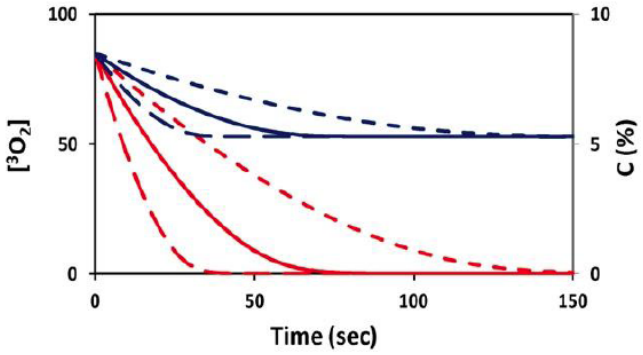

Figure 3: The time profiles of oxygen, $[O_2]$, and photosensitizer concentration, C(z,t), for various light intensity of I_0= (50,100, 200) mW/cm^2, (for curve from top to low), for k_6/k_{12}=1,000, $k_{83}=(k_8/k_3)$=0.0001, b'=aq=0.003, $[A]_0$=50, and d'=33 uM, for P=0 and at z=0; where red and blue curves are for oxygen and photosensitizer concentration, respectively.

From the profiles (shown in Figures **3** to **5**) of $[^3O_2]$, C(z,t) and S2 function for various parameters (I_0, C_0, k_{83}, [A], P), the important features of anti-cancer are summarized as follows:

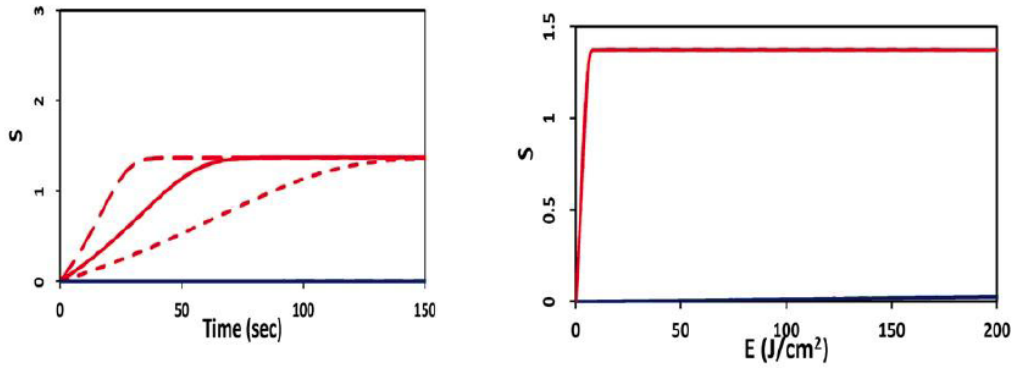

Figure 4: The S2 function associate to Figure **3**, showing S2 versus time (t) for light intensity of I_0= (50,100, 200) mW/cm^2, (for curve from left to right); and S2 versus fluence, where all the curves overlap to one for the case of P=0.

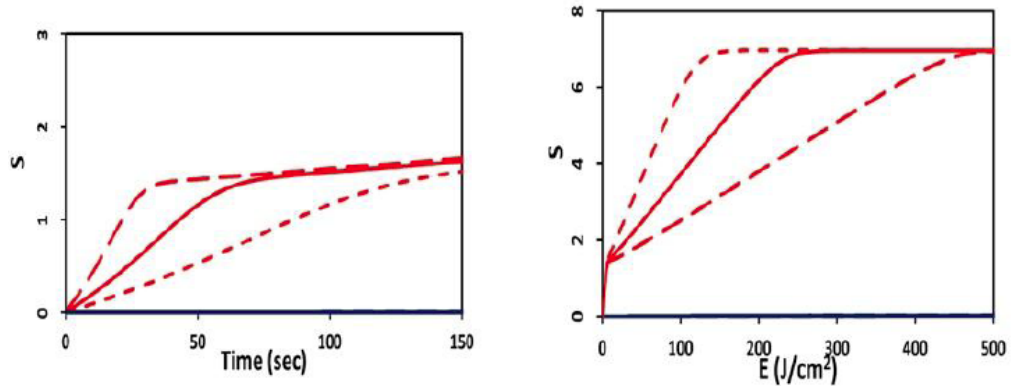

Figure 5: Same as Figure **4**, but for P=0.07 (uM/s).

(a) Both T1 and T2 are decreasing function of the light intensity, that is higher intensity has smaller T1 and T2, whereas it has faster rising profile of the S-functions.

(b) For small rate constants $k_{83}=k_8/k_3=0.001$, type-II is dominant over type-I, where increasing of k_{83} will reduce the value of S2 due to the reduction of K'.

(c) Higher intensity depletes [$^3O_2$] and C(z,t) faster such that it produces higher singlet oxygen [$^1O_2$] and has higher efficacy, in the transient state. However, they reach the same steady-state efficacy (or S function).

(d) As shown by Figure **4**, for S2 versus fluence, all the curves overlap to one, for the case of P=0, and follow the BRL; whereas they follow a nonlinear law when P>0 (as shown by Figure **5**); and higher intensity needs a larger fluence to achieve the same efficacy as that of lower intensity. Under the BRL (when P=0), the S-E curves overlap for various intensity (with the same dose), i.e., same dose achieves same efficacy and independent to the intensity.

(e) Figure **5** also shows higher efficacy when there is oxygen supply (with P>0), since the S2 function is proportional to the time integral of C[O_2].

CONCLUSION

Efficacy of cancer therapy may be enhanced by the oxygen source term. To achieve the same efficacy, minimum dose and/or less exposure time for accelerated procedure may be achieved by using a higher intensity (but same dose) for the case of P=0. However, with P>0, higher intensity requires a higher fluence to achieve the same efficacy and it does not follow the BRL reciprocity law.

CONFLICT OF INTEREST

One of the authors (JT Lin) is the CEO of New Vision Inc. and has financial interest.

ACKNOWLEDGEMENTS

This work was supported by the internal grant of New Vision Inc, and also partially supported by a grant from Talent-Xiamen (XM-200) program (Xiamen

Science & Technology Bureau, China). KT Chen is partially supported by the Ph.D program of Graduate Institute of Applied Science and Engineering, Fu Jen Catholic University, Taiwan.

REFERENCES

[1] Lin JT, Chen KT, Liu HW. Progress of nanotechnology for phototherapy: Fundamentals and Applications. Med Devices Diagn Eng 2017. https://doi.org/10.15761/MDDE.1000124

[2] Lin JT, Chiang S, Lin GH, *et al*. *In vitro* photothermal destruction of cancer cells using gold nanorods and pulsed-train near-infrared lase. J Nanomaterials 2012; article ID 861385. https://doi.org/10.1155/2012/861385

[3] Lin JT. Analysis of the efficiency of photothermal and photodynamic cancer therapy via nanogolds and photosensitizers. J Cancer Research Update 2017: 12-18. https://doi.org/10.6000/1929-2279.2017.06.01.2

[4] Choi SS, Lee HK, Chae HS. Synergistic *in vitro* photodynamic antimicrobial activity of methylene blue and chitosan against Helicobacter pylori 26695 Photodiag Photodany Therapy 2014; 11: 526-532.

[5] Wang YH, Chen SP, Liao AH, *et al*. Synergic delivery of gold nanorods using multifunctional microsbubbles for enhanced plasmonic photothermal therapy. Scientific Report 2014: 5685. doi:10.1038/srep0585.

[6] Shirata C, Kaneko J, Inagaki Y, *et al*. Near-infrared photothermal/photodynamic therapy with indocyanine green induces apoptosis of hepatocellular carcinoma cells through oxidative stress. Scientific Reports 2017; 7. Article number: 13958. https://doi.org/10.1038/s41598-017-14401-0

[7] Lin JT. Lin-scaling-laws for optimal efficacy in photo-biological systems versus Arndt-Schulz-Law and Bunsen-Roscoe law. Med Devices Diagn Eng 2018; 3: 120-13. doi: 10.15761/MDDE.1000125.

[8] Lin JT. Efficacy S-formula and kinetics of oxygen-mediated (type-II) and non-oxygen-mediated (type-I) corneal cross-linking. Ophthalmology Research 2018; 8(1): 1-11. Article no.OR.39089. DOI : 10.9734/OR/2018/39089.

[9] Foster TH, Murant RS, Bryant RG, *et al*, Oxygen consumption and diffusion effects in photodynamic therapy. Radiat Res 1991; 126: 296-303. [PubMed] https://doi.org/10.2307/3577919

[10] Hu XH, Feng Y, Lu JQ, *et al*. Modeling of a Type II photofrin-mediated photodynamic therapy process in a heterogeneous tissue thantom. Photochem Photobiol 2005; 81: 1460-1468. [PubMed] https://doi.org/10.1562/2005-05-04-RA-513

[11] Wang KKH, Finlay JC, Busch TM, *et al*. Explicit dosimetry for photodynamic therapy: macroscopic singlet oxygen modeling. Journal of Biophotonics 2010; 3(5-6): 304-318. [PubMed: 20222102]. https://doi.org/10.1002/jbio.200900101

[12] Zhu TC, Finlay JC, Zhou X, *et al*. Macroscopic modeling of the singlet oxygen production during PDT. Proc SPIE 2007; 6427: 6427O81-6427O812.

[13] Zhu TC, Kim MM, Ong YH, *et al*. A summary of light dose distribution using an IR navigation system for Photofrin-mediated pleural PDT. Proc SPIE 2017; 10047. https://doi.org/10.1117/12.2253027

Received on 26-02-2018 Accepted on 28-02-2018 Published on 28-02-2018

DOI: http://dx.doi.org/10.6000/1929-2279.2018.07.01.2